Analysis, Design, and Implementation of a Single-Phase Power-Factor Corrected AC-DC Zeta Converter with High Frequency Isolation

Bhim Singh†, Mahima Agrawal*, and Sanjeet Dwivedi**

Abstract – This paper deals with the analysis, design, and implementation of a single phase AC-DC Zeta converter with high frequency transformer isolation and power factor correction (PFC) in two modes of operation, discontinuous current mode of operation (DCM), and continuous current mode of operation (CCM). A Digital Signal Processor (DSP) based implementation is carried out for validation of the Zeta converter developed design in discontinuous mode of operation. A comparison of both modes of operation is presented for a 1kW power rating from the point of view of steady state and dynamic behavior, power quality, simplicity, control technique, device rating, and converter size. The experimental results of a developed prototype of Zeta converter are presented for validation of the developed design. It is observed that CCM is most suitable for higher power applications where it requires some complex control and sensing of the additional variables.

Keywords: AC-DC converter, CCM, DCM, Digital Signal Processor (DSP), Power-factor correction (PFC), Zeta converter

1. Introduction

The conventional technique of AC-DC conversion using a diode rectifier with bulk capacitor is no longer in use due to numerous problems such as low order harmonics injection into AC power supply, low power factor, high peak current, line voltage distortion, increased electromagnetic interference, extra burden on lines, and additional losses [1]. Many new topologies have been introduced which not only overcome these drawbacks, but establish some attractive features for AC-DC rectification with different level output voltages. A boost converter is most widely used for this purpose due to its simple circuitry and easy control, which can be implemented effortlessly with available ICs. However, some applications require the high frequency isolation with various levels of output voltage. In recent years, single stage AC-DC power converters such as Flyback, Cuk, SEPIC, and Zeta converters have been widely used for PFC where drawbacks of the boost converter are nicely addressed [1-10].

A Zeta converter lacks wide attention and available literature is limited. The discontinuous conduction mode of the converter is nicely presented in [2]. Some authors [3-8] have also discussed its continuous conduction mode. The purpose of this paper is to present the operation and behavior of the Zeta converter in continuous and discontinuous conduction mode with two distinct control methods, voltage follower and average current mode control for DCM and CCM respectively, and to analyze the converter operation and performance of a Zeta converter in detail from various points of view in both modes.

† Corresponding Author: Department of Electrical Engineering, Indian Institute of Technology, Delhi, Hauz Khas, New Delhi 110 016, India. (bsingh@ee.iitd.ac.in)
* APC Bangalore (mahima.agarwal@apcc.com)
** Dept. of Electrical Engineering, Indira Gandhi Government Engg. College, Sagar, MP-470004, India. (sanjeetkd@gmail.com)
Received 3 September, 2007; Accepted 11 April, 2008

2. Analysis and Control of Zeta Converter in DCM

In this section, operation and control of a Zeta converter in DCM mode is analyzed.

2.1 Analysis of Zeta Converter in DCM

A Zeta converter with high frequency transformer isolation is shown in Fig. 1a. The switching frequency is considered much higher than line frequency so that averaged quantities over a switching cycle can be considered in place of instantaneous quantities.

Three equivalent circuits for DCM are shown in Figs. 1b(i), (ii), and (iii) for three stages of operations. DCM introduces a third switching stage in which the sum of transformer magnetizing current is referred to the secondary side of the transformer and output inductor current is zero for a specified period before the beginning of the next cycle. Thus diode current approaches zero and the converter enters discontinuous conduction mode. Fig. 1c shows the ideal waveforms for voltage and current of the magnetizing inductance and output inductors in DCM.

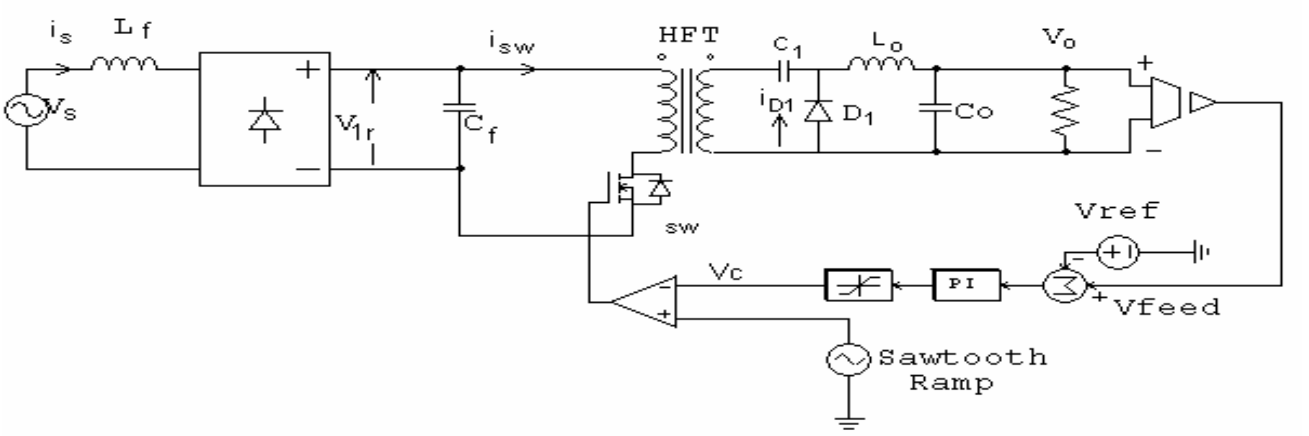

Fig. 1a. Single-Phase Buck-Boost Zeta AC-DC Converter in DCM.

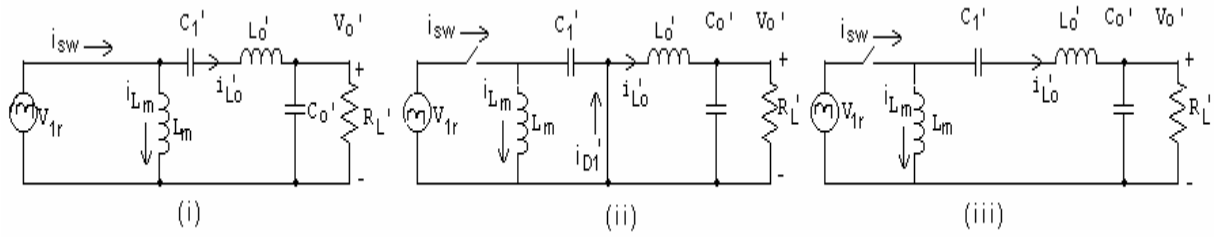

Fig. 1b. Switching networks of Zeta converter in DCM.

To simplify the analysis, all quantities are referred to the primary side of the transformer. The volt-second balance gives the following equality:

$$\frac{v_o'}{v_{1r}} = \frac{d}{d_1} \tag{1}$$

where v_o' and v_{1r} are output voltage (referred to primary) and rectified input voltage, respectively. The d is the duty ratio and d_1T_s is the diode conduction period, during which inductor currents decrease linearly.

Assuming 100% efficiency for simplification, the current ratio is:

$$\frac{i_m}{i_{Lo'}} = \frac{d}{d_1} \tag{2}$$

where i_m and i_{Lo}' are the magnetizing current and output inductor current referred to in the primary side of the transformer.

First Stage of Operation

When the switch is on, currents through the magnetizing inductance and the output inductor increase linearly with the voltage across them equal to the input voltage. The equations of magnetizing and output inductor currents for the interval $0<t<dT_s$ (referring to Fig. 1b (i)) are given as:

$$i_m = i + \frac{v_{1r}}{L_m} t \tag{3}$$

$$i_{Lo}' = -i + \frac{v_{1r}}{L_o'} t \tag{4}$$

where i is the minimum input inductor current. L_m and L_o' are magnetizing inductance and output inductor referred to in the primary side, respectively.

Second Stage of Operation

When the switch is off, the two inductor currents decrease linearly with the voltage across them equal to output voltage. Referring to Fig. 1b(ii) and Fig. 1c, inductor currents are given as:

$$i_m = -\frac{v_o'}{L_m} t + \frac{v_{1r}}{L_m} dT_s + i \tag{5}$$

$$i_{Lo}' = -\frac{v_o'}{L_o'} t + \frac{v_{1r}}{L_o'} dT_s - i \tag{6}$$

Third Stage of Operation

This is the stage when the diode current is zero. Averaged input and output inductor currents over a switching period can be given as:

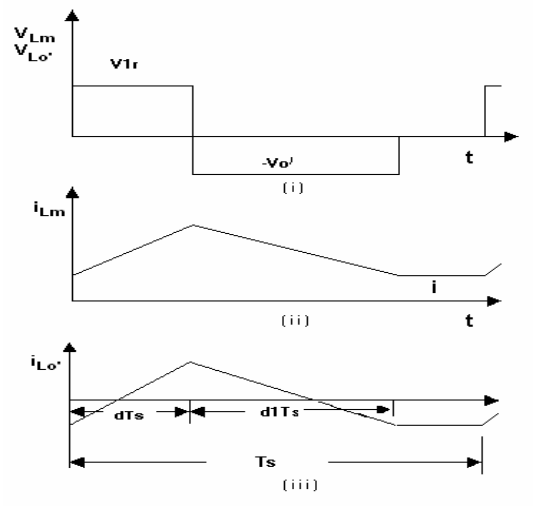

Fig. 1c. Inductor voltages and current waveforms in Zeta converter in DCM.

$$i_m = \frac{v_{1r}}{2L_m} dT_s (d+d_1) + i \tag{7}$$

$$i_{Lo}' = \frac{v_{1r}}{2L_o'} dT_s (d+d_1) - i \tag{8}$$

Sum of the input and output inductor currents is given as:

$$i_m + i_{Lo}' = \frac{1}{2} \frac{v_{1r}}{L_{eq}} dT_s \left(1+\frac{d_1}{d}\right) d \tag{9}$$

where,

$$L_{eq} = \frac{L_m L_o'}{L_m + L_o'} \tag{10}$$

By substituting the expression in Eqn. (2) into Eqn. (9), one gets:

$$i_m \left(1+\frac{d_1}{d}\right) = \frac{1}{2} \frac{v_{1r}}{L_{eq}} dT_s \left(1+\frac{d_1}{d}\right) d \tag{11}$$

After simplification it gives:

$$i_m = \frac{v_{1r} d^2 T_s}{2L_{eq}} \tag{12}$$

It can be written as:

$$i_m = I_1 \left| \sin \omega t \right| \tag{13}$$

where,

$$v_{1r} = V_1 \left| \sin \omega t \right| \tag{14}$$

$$I_1 = \frac{V_1 d^2 T_s}{2L_{eq}} \tag{15}$$

since the average current of energy transfer capacitor (C_1) is zero. Therefore average input current is the average magnetizing current, thus from Eqn. (13), it is clear that by keeping the duty cycle and switching frequency constant, the average input current in the Zeta converter in DCM follows the input voltage exactly thus emulating a resistor and this is known as voltage follower technique. Therefore, the Zeta converter behaves as an ideal current shaper, and performs current shaping automatically with no control when operating in DCM.

2.2 Control Technique of Zeta Converter in DCM

In DCM, the voltage follower approach is applied for the PWM control of the converter. The operation of the Zeta converter in DCM uses a simple control technique, which requires sensing of output voltage only. There is only one control loop and no current feedback is required, thus making the control technique simpler and known as voltage follower approach.

The output voltage regulation is provided by the feedback loop as shown in Fig. 1a, where the output voltage is compared with a reference V_{ref} value and the error is amplified in a P-I controller which is further compared with a saw-tooth ramp V_s, thus providing the pulses to power switch. The control provides regulated output voltage with automatic current shaping where the voltage regulation is provided by controlling duty ratio d and current shaping is achieved by emulating a resistor where duty ratio and emulated resistor are both functions of control signal V_c.

3. Analysis and Control of Zeta Converter in CCM

In this section, operation and control of the Zeta converter in CCM mode is analyzed.

3.1 Analysis of Zeta Converter in CCM

Figs. 2a, 2b, and 2c show the control technique, switching networks, and voltage and current waveforms of the magnetizing inductance as well as an output inductor, respectively in CCM. The operation of a Zeta converter in CCM is analyzed with the help of a switching network shown in Figs. 2b(i), (ii) for various modes of operation.

First Stage of Operation

It begins when the switch is turned on at t = 0, the equivalent circuit of which is indicated in Fig. 2b(i). The currents in magnetizing and output inductors rise linearly with voltage across them equal to input voltage.

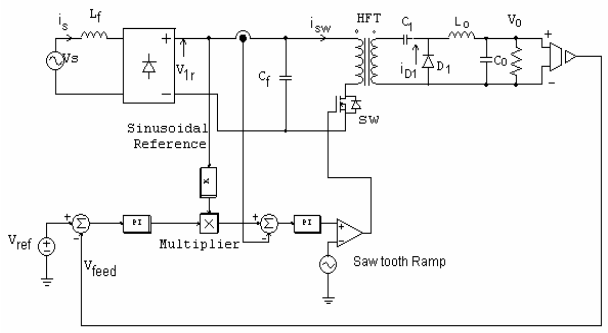

Fig. 2a. Average current control of Zeta AC-DC converter for CCM operation.

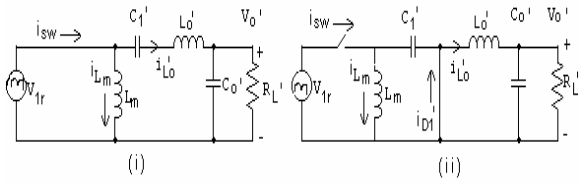

Fig. 2b. Switching Networks of Zeta Converter in CCM.

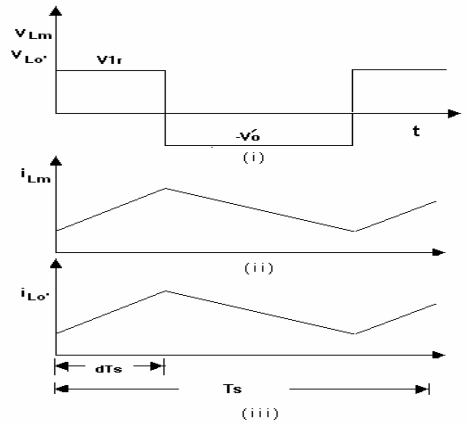

Fig. 2c. Inductors voltage and current waveform Zeta converter in CCM.

Second Stage of Operation

It begins when the switch is turned off. The equivalent circuit is shown in Fig. 2b(ii). In this mode, capacitors C_1 and C_o are charged through L_m and L_o respectively, thus two inductor currents start decreasing linearly. CCM mode is analyzed.

3.2 Control Techniques of Zeta Converter in CCM

Fig. 2a shows the circuit diagram of the buck-boost PFC Zeta converter circuit with average current mode control. It includes an inner current loop and an outer voltage loop. The PFC is achieved by tracking the average current to a reference value generated by multiplying the output of voltage error amplifier and a fraction of rectified input voltage. Clearly, this is a complex control scheme with additional variable sensing requirements.

4. Design of Zeta Converter in DCM and CCM

The design of the Zeta converter can be obtained by considering it as a DC-DC converter in very special conditions where the input DC voltage varies continuously during the line cycles with the output voltage being constant. The design procedure is presented here for both modes of operation.

The design of the converter depends whether it is working in discontinuous or continuous conduction mode. The transfer function of the Zeta converter in DCM is given as:

$$\frac{v_o}{v_{1r}} = \frac{d}{d_1 n} \tag{16}$$

where n is the turn ratio. From Fig. 1b, for DCM operation,

$$d+d_1<1 \tag{17}$$

From Eqns. (16) and (17) for the desired maximum duty ratio at minimum input voltage, the turn ratio can be obtained by satisfying the following inequality,

$$n>\frac{d}{(1-d_1)}\frac{V_1}{V_o} \tag{18}$$

However, it also affects the voltage stress across the switch. Thus a compromise is made between d_{max} and voltage stress across the switch to get the turn ratio.

The transformer magnetizing inductance is an important factor in deciding the mode of operation. The mode of operation depends upon the equivalent inductance L_{eq}, which is the parallel combination of the magnetizing inductance and an output inductance. However, the output inductor has a reasonable effect on output voltage ripple, thus it is significantly larger than the magnetizing inductance and thus the mode of operation mainly depends upon magnetizing inductance. In order to ensure DCM at maximum load, the following condition must be satisfied:

$$L_{eq}<\frac{R_{Lmin}(1-d)^2}{2f_s} \tag{19}$$

where R_{Lmin} is the minimum value of the load resistance and f_s is the switching frequency.

The output inductor, L_o is selected on the basis of maximum ripple allowed in the output current.

$$L_o=\frac{V_{1r}d}{f_s\Delta i_{Lo}} \tag{20}$$

where Δi_{Lo} is the ripple in the output current in Amperes.

Once L_o is determined, the magnetizing inductance of the transformer is found by Eqn. (19) and the following equality:

$$L_m=\frac{L_{eq}L_o'}{L_o'-L_{eq}} \tag{21}$$

The output capacitor is selected on the basis of maximum peak-to-peak ripple in output voltage (r_v) as:

$$C_o > \frac{V_o}{r_v \omega R_L} \tag{22}$$

An input filter is required to reduce the ripple in the input current. A large value of input capacitor distorts input current waveform as the current becomes discontinuous due to the fact that reactive energy of capacitor C_f cannot be fed back to input supply in the presence of a unidirectional diode bridge. Thus a small value of an input filter capacitor should be selected.

For the CCM, the transfer function is given as:

$$V_o = \frac{dv_{1r}}{(1\text{-}d)n} \tag{23}$$

Thus in a similar manner as in DCM, for desirable maximum duty ratio, turn ratio is determined. However, equivalent inductance of the transformer is defined by satisfying the following inequality [6]:

$$L_{eq} > \frac{R_{Lmax}(1\text{-}d)^2}{2f_s} \tag{24}$$

Other components are designed in a similar manner as in DCM. For both modes of operation,

The peak voltage across the switch is given as:

$$V_{swpk} = V_1 + nV_o \tag{25}$$

The peak voltage across the diode can be given as:

$$V_{diopk} = \frac{V_1}{n} + V_o \tag{26}$$

However, the leakage inductance causes high voltage spikes across the devices, which should be taken into consideration in device selection.

5. Results and Discussion

In order to demonstrate the converter performance in both modes of operation of DCM and CCM, a 1kW converter prototype is designed with the following specifications:

Input: $V_1 = 220V_{RMS}$, 50Hz, Single-Phase AC Supply

Output: $V_o = 48V, P_o = 1kW$, output voltage-ripple less than 2%

Switching frequency $f_S = (\omega_S / 2\pi) = 50kHz$

Following the design procedure presented above, the converter parameters for DCM are:

Transformer turn ratio (n) 5:1, Magnetizing inductance L_m=100μH, L_o=10mH, C_1=10μF, C_o=22mF, L_f=3mH and C_f=100nF.

5.1 Simulation Results

A simulation is performed for both modes of operation using PSIM software, which is a CAD software package, developed specifically for power electronics and applications of motor drives. Fig. 3a shows the source voltage and source current for full load condition (1kW) in DCM. From these curves and Table I, it is clear that the input current follows the input voltage and the circuit behaves as a resistor emulator. The THD of the input current is observed to be 4.98% in DCM. A reasonably high power factor is achieved of the order of 0.9975 at full load in DCM. Fig. 3b displays the harmonic spectrum of the source current. From this figure, it can be observed that harmonic currents are reduced resulting in high level of power quality at AC mains. The steady state output voltage is presented in Fig. 3c in which the output voltage ripple is observed to be about 1.99% at full load.

The switch voltage and its current are shown in Fig. 3d for full load condition in DCM. Here, an important point to note is the occurrence of a high level of stress (28A) on the device in DCM. Normalizing the device peak current to the peak of the source current, its normalized value is 4.15pu, which is quite high. Fig. 4a displays source voltage and source current for 10% loading condition (100W) in which the THD of AC current is about 11%. The source current harmonic spectrum at 10% load in DCM is shown in Fig. 4b. In order to study the control loop functionality and dynamic behavior of the converter, the source voltage and source current are revealed in Fig. 5a for the sudden application of 100% load and then removal of load (10%-100%-10% load change) in DCM. The output voltage and current are shown in Fig. 5b.

Similarly, the Zeta converter with identical specifications is designed in CCM. The designed parameters for CCM are as follows:

Transformer turn ratio (n) 5:1, Magnetizing inductance L_m=2mH, L_o=8mH, C_1=10μF, C_o=22mF, L_f=5mH and C_f=150nF.

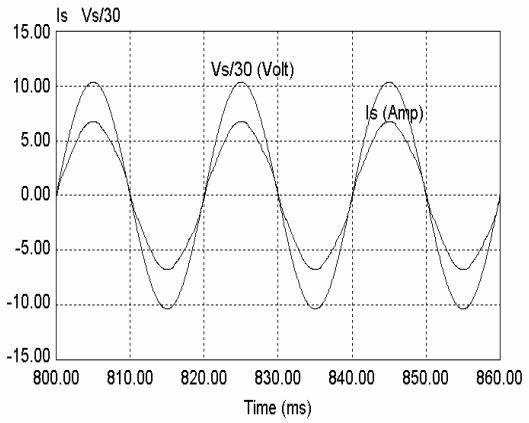

Fig. 3a. Source voltage and current in DCM at 100% load.

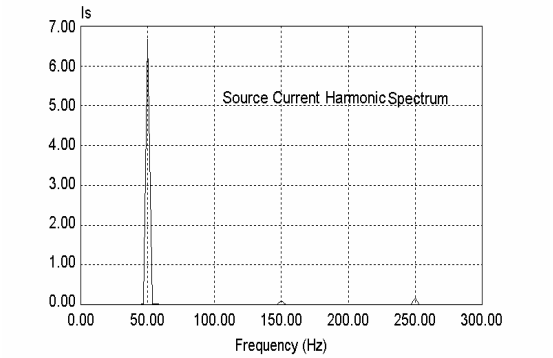

Fig. 3b. Harmonic spectrum of source current in DCM at 100% load.

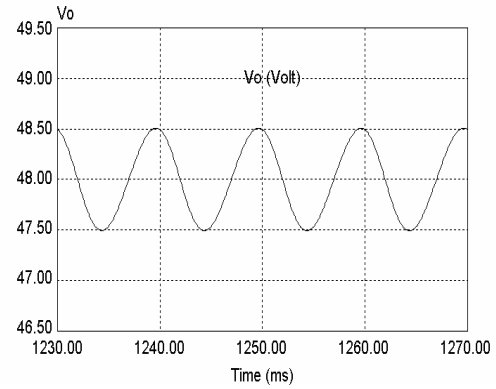

Fig. 3c. Steady state output voltage in DCM at 100% load.

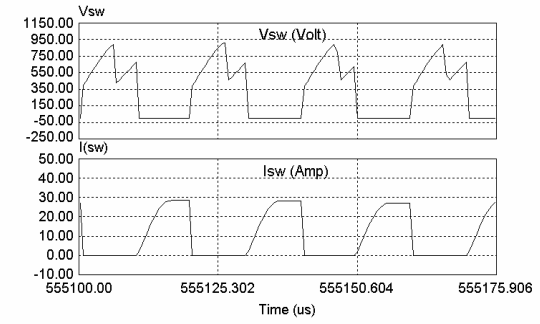

Fig. 3d. Switch voltage and switch current in DCM at 100% load.

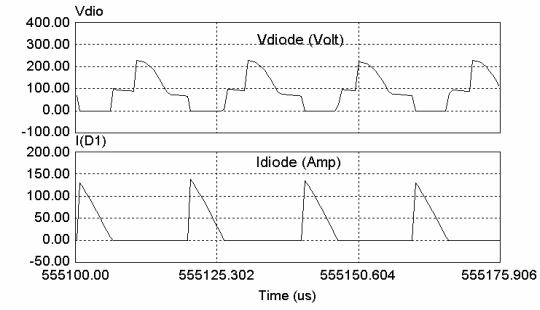

Fig. 3e. Diode voltage and diode current in DCM at 100% load.

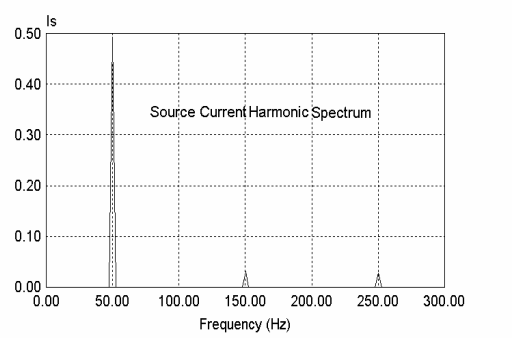

Fig. 4a. Source voltage and current in DCM at 10% load.

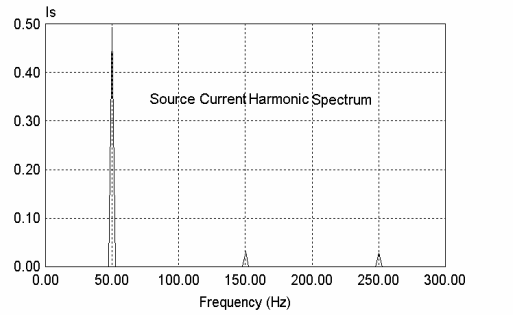

Fig. 4b. Harmonic spectrum of source current in DCM at 10% load.

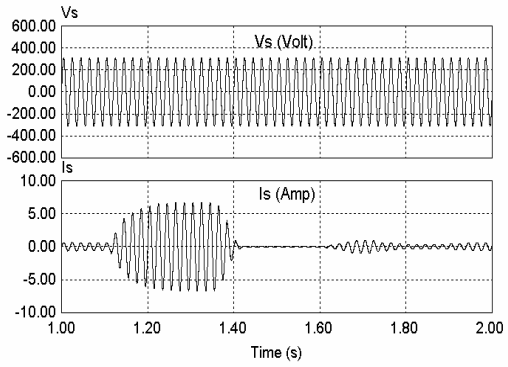

Fig. 5a. Source voltage and current in DCM for load application and removal (10%-100%-10%).

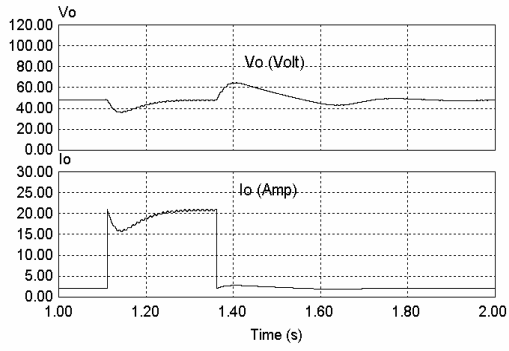

Fig. 5b. Output voltage and current in DCM for load application and removal (10%-100%-10%).

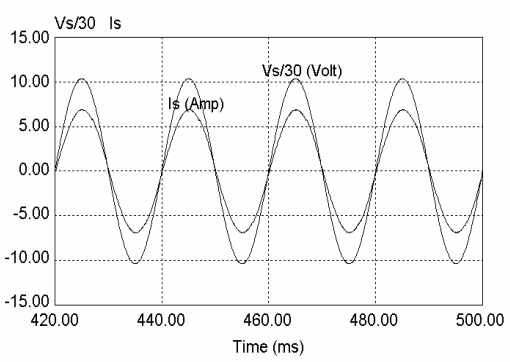

Fig. 6a. Source voltage and current for 100% load in CCM.

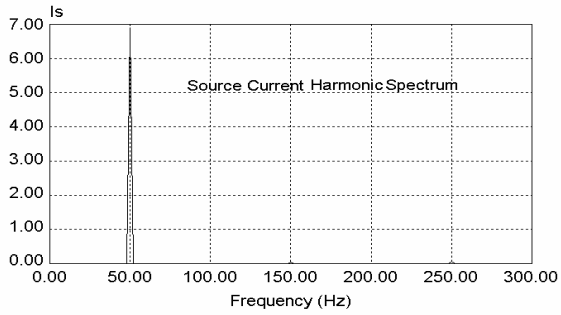

Fig. 6b. Source current harmonic spectrum for 100% load in CCM.

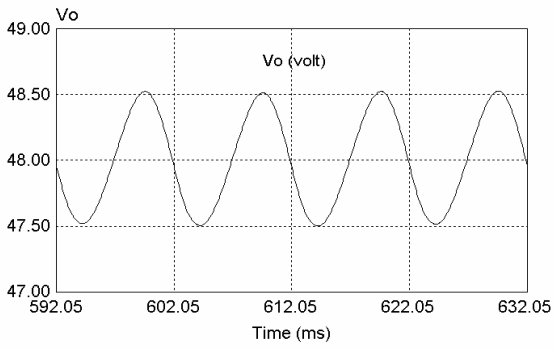

Fig. 6c. Steady state output voltage in CCM at 100% load.

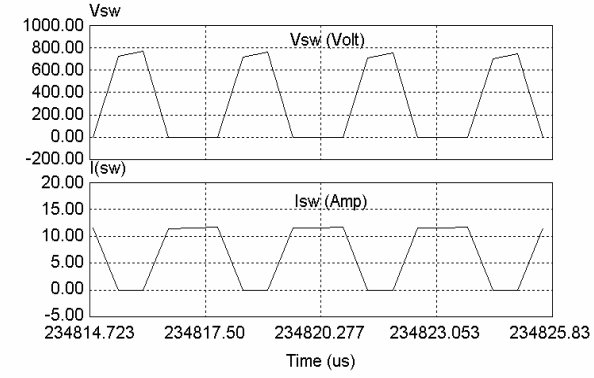

Fig. 6d. Switch voltage and switch current in CCM at 100% load.

Simulation results are presented in Figs. 6a-6e and Table I for CCM at full load (1kW) to demonstrate the power quality. Fig. 6a shows the source voltage and source current for full load condition in CCM. The THD of the input current is observed to be 1.36% and the power factor is around 0.998, which is quite high. Fig. 6b displays the harmonic spectrum of the source current, which shows the presence of a small magnitude of third harmonics in the input current.

The steady state output voltage at full load condition in CCM is shown in Fig. 6c. The output voltage ripple is observed to be 1.98%. Fig. 6d indicates voltage across the switch and current through the switch in CCM.

The peak current through switching device is observed to be 12A. Normalizing it to source peak current, its normalized value is 1.75 pu, which is quite low in comparison to 4.15 pu in DCM as shown in Table I. The diode peak current in CCM is 60A as indicated in Fig. 6e as compared to 135A in DCM. Fig. 7a presents source voltage and source current for 10% loading condition (100W) in CCM. The THD of source current is about 9.2%. Fig. 7b displays the source current harmonic spectrum at 10% load in CCM. Dynamic performance of the converter is observed under application and removal of load (10%-100%-10% load change) in CCM as revealed in Figs. 8a and 8b. From these results, it can be observed that there is little difference in output voltage on application of the load, which recovers in a few cycles due to the action of a closed loop controller. Moreover, the control action in CCM is better than in DCM in view of voltage regulation as well as fast response with load changes. However, size of the converter in CCM is larger than in DCM where it requires smaller magnetizing inductance and other components.

Various waveforms given for DCM and CCM clearly dictate that DCM imposes very high switching device stresses (4.15pu) as compared to CCM, where the device rating is significantly reduced (1.75pu).

Before making the final conclusion, it would be better to discuss the features and requirements of the converter. The power level specified in this case is sufficiently high (1kW). In addition some overload capacity is also provided. It should also give good performance in the wide operating range i.e. from 10% to 100% loading conditions. From these results and observations, it is clear that for higher power application, an input current THD, power factor, and ripple factor are superior in CCM than in DCM operation. Moreover, for such a high power operation, the device stresses in DCM are much higher. The CCM provides all the benefits of the current control as compared to the voltage mode such as improved dynamic performance and enhanced line regulation, etc. However, in view of simple control, reduced sensing requirement, circuit simplicity and size of the converter, the DCM is better than the CCM which can easily be used in small power applications.

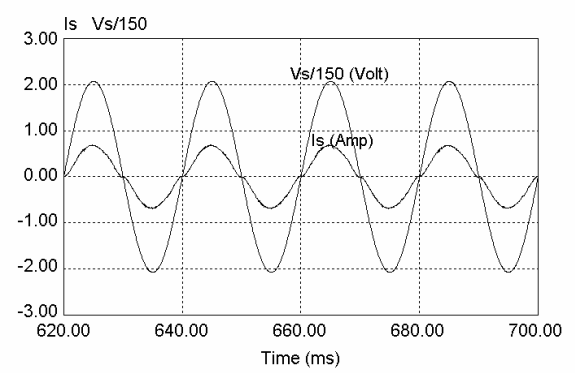

Fig. 7a. Source voltage and current in CCM at 10% load.

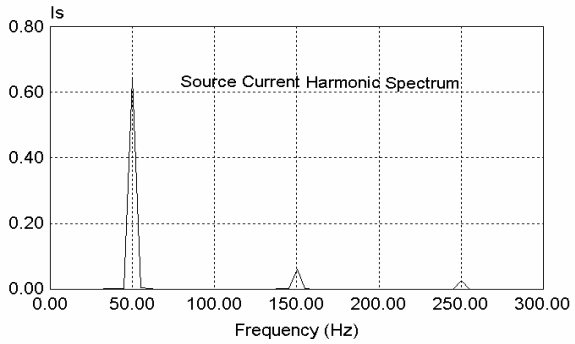

Fig. 7b. Source current harmonic spectrum in CCM at 10% load.

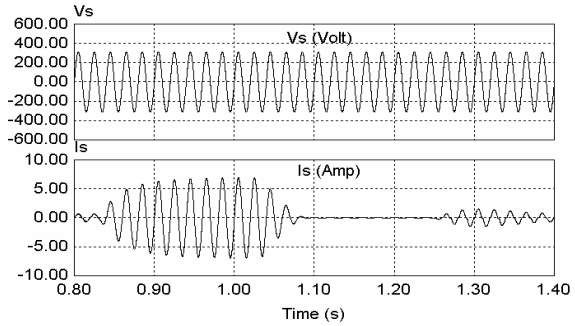

Fig. 8a. Source voltage and current in CCM for load application and removal (10%-100%-10%).

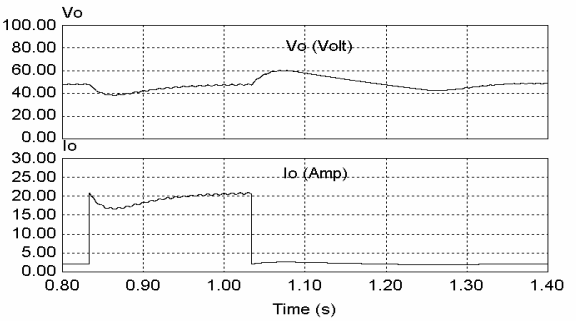

Fig. 8b. Output voltage and current in CCM for load application and removal (10%-100%-10%).

5.2 Experimental Validation

The test results are obtained from the developed transformer isolated AC-DC Zeta converter. The experimental setup used for the validation of developed design in DCM of operation is shown in Fig. 9. The performance of a Zeta converter and power quality at AC mains is observed with 200W resistive load and it is shown in Figs. 10a-b for the sudden application and removal of resistive load. Figs. 11a-b show the steady state performance of a Zeta converter feeding the equivalent resistive load of 60W. The harmonic spectra of AC mains current are presented in Figs. 12a-b for an AC-DC Zeta converter feeding the equivalent resistive load of 200W. The experimental results verify simulated results and thus validate the developed design and simulation model of a transformer isolated AC-DC Zeta converter in DCM of operation for improving the power quality at AC mains.

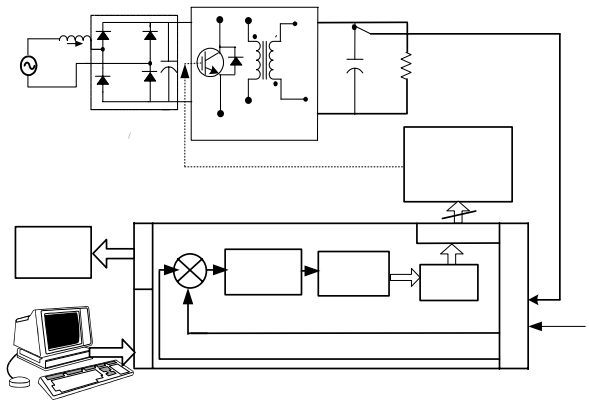

Fig. 9. Experimental setup for DSP based implementation of a High Frequency Transformer Isolated AC-DC Zeta converter.

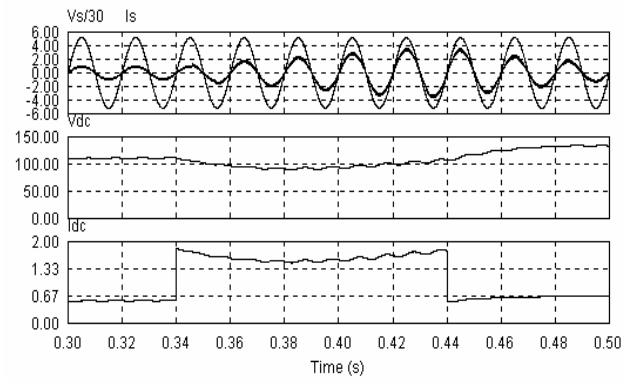

Fig. 10a. Simulated responses of AC mains voltage, AC mains current, output DC voltage, and output DC current waveform of AC-DC Zeta converter for load perturbation response on equivalent resistive load (60W to 200W to 60W).

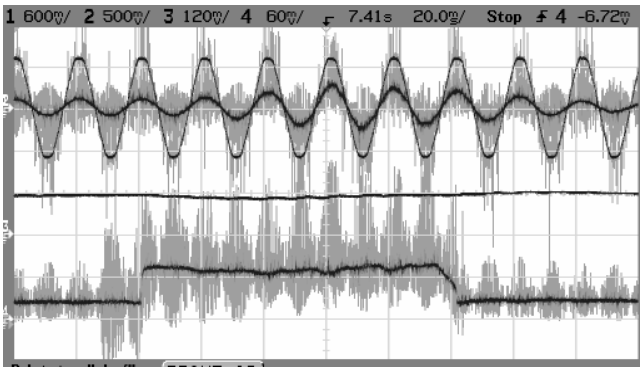

Fig. 10b. Test results of AC mains voltage, AC mains current, output DC voltage and output DC current waveform of AC-DC Zeta converter for load perturbation response on equivalent resistive load (60W to 200W to 60W). (Scale on X-axis 1div=20ms, Y-axis channel-1 1div =150V, channel-2 1div =3A, channel-3 1div= 100V, channel-4 1div= 1.75A).

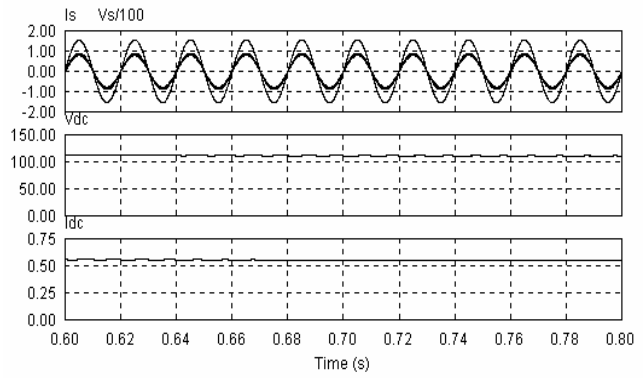

Fig. 11a. Simulated results of AC mains voltage, AC mains current, output DC voltage and output DC current waveform of AC-DC Zeta converter for steady state response on equivalent resistive load (60W).

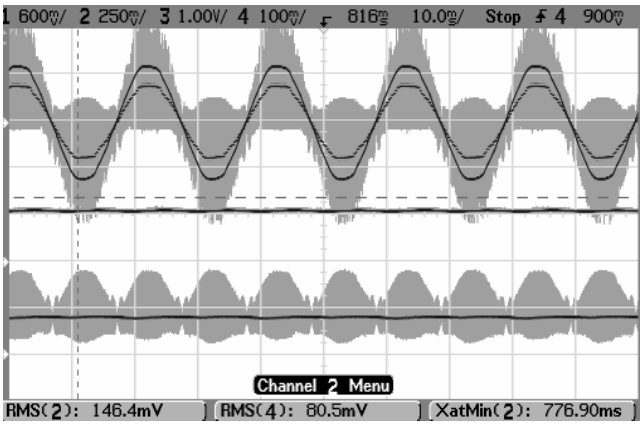

Fig. 11b. Test results of AC mains voltage, AC mains current, output DC voltage and output DC current waveform of AC-DC Zeta converter for steady state response on equivalent resistive load (60W). (Scale on X-axis 1div=10ms, Y-axis channel-1 1div =160V, channel-2 1div =1A, channel-3 1div= 100V, channel-4 1div= 1.5A).

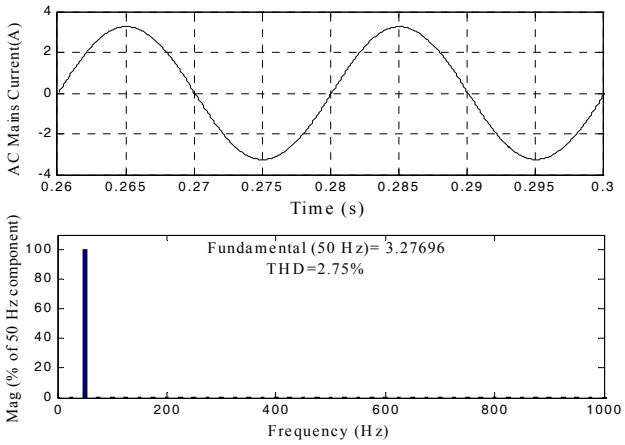

Fig. 12a. Harmonic spectrum of AC mains current for AC-DC Zeta converter feeding the equivalent resistive load (200W).

Table 1. Comparisons of Zeta Converter Operation in DCM and CCM

Quantity		DCM Operation		CCM Operation	
		10% Load	100% Load	10% Load	100% Load
Input Current THD		11%	4.98%	9.2%	1.36%
PF		0.993	0.9975	0.994	0.998
Output Ripple		0.62%	1.99%	0.67%	1.98%
Normalized Current of Switch	Peak	9.21	4.15	2.92	1.75
	Average	0.92	1.01	0.45	0.62
	RMS	2.15	1.71	1.04	0.95
Normalized Current of Diode	Peak	36.90	20.01	14.6	8.73
	Average	4.52	3.02	3.24	3.17
	RMS	10.45	5.41	5.37	4.57
Control Technique		Voltage Mode Control		Average Current Control	
Size of Converter		Small		Large	
Circuit Simplicity		Simple		Complex	

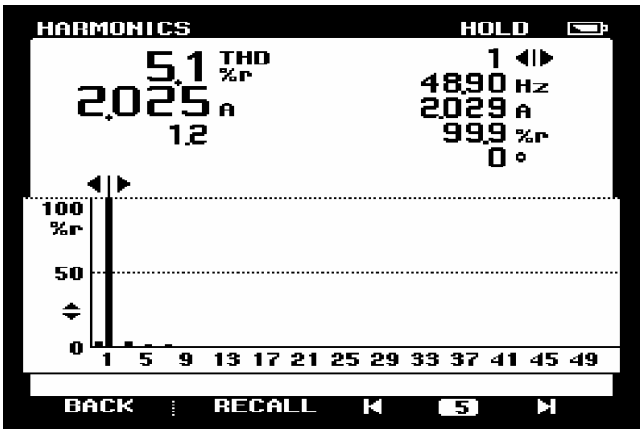

Fig. 12b. Harmonic spectrum of AC mains current for AC-DC Zeta converter feeding the equivalent resistive load (200W).

5. Conclusion

The analysis, design, and DSP based implementation of an AC-DC Zeta converter have been carried out to demonstrate power quality improvement in both modes of operation, namely DCM and CCM. The DCM plays an important role with simple control technique in AC-DC conversion with high level of power quality in low power applications. However, for high power applications, the CCM of a Zeta converter is most suitable due to less device stresses and improved performance.

References

[1] M. Brkovic and S. Cuk, "Input current shaper using Cuk converter," in *Proc. IEEE INTELEC*, 1992, pp. 532-539.

[2] A. Peres, D.C. Martins, and I. Barbi, "ZETA converter applied in power factor correction," in *Proc. IEEE PESC*, 1994, pp. 1152-1157.

[3] D. C. Martins and G. N. de Abreu, "Application of the ZETA converter in switched-mode power supplies," in *Proc. IEEE Power Conversion Conference*, 1993, pp. 147-152.

[4] D. C. Martins, F. de Souza Campos, and I. Barbi, "ZETA converter with high power factor operating in continuous conduction mode," in *Proc. IEEE INTELEC*, 1996, pp. 107-113.

[5] D. C. Martins, F. de Souza Campos, and I. Barbi, "ZETA converter with high power factor operating in continuous conduction mode," in *Proc. IEEE IECON*, 1996, pp. 1802-1807.

[6] D. C. Martins and G. N. de Abreu, "Application of the ZETA converter in switched-mode power supplies," in *Proc. IEEE APEC*, 1993, pp. 214-220.

[7] D. C. Martins and M. M. Casaro, "Isolated three-phase rectifier with high power factor using the Zeta converter in continuous conduction mode," *IEEE Trans. Circuits and Systems I: Fundamental Theory and Applications,* vol. 48, pp. 74 - 80, Jan. 2001.

[8] D. C. Martins, M. M. Casaro and I. Barbi, "Isolated three-phase rectifier with high power factor using the Zeta converter in continuous conduction mode," in *Proc. IEEE INTELEC*, 1997, pp. 331-337.

[9] H. Wei and I. Batarseh, "Comparison of basic converter topologies for power factor correction," in *Proc. IEEE Southeastcon*, 1998, pp. 348-353.

[10] B. Singh, B. N. Singh, A. Chandra, K. Al-Haddad, A. Pandey, and D. P. Kothari, "A review of single-phase improved power quality AC-DC converters," *IEEE Trans. Industrial Electronics,* vol. 50, no. 1, pp. 962-981, Oct. 2003.

Bhim Singh

He was born in Rahamapur (U.P.), India in 1956. He received his B.E. (Electrical) degree from the University of Roorkee, Roorkee, India in 1977 and his M.Tech. and Ph.D. degrees from the Indian Institute of Technology (IIT), New Delhi, India in 1979 and 1983, respectively.

In 1983, he joined the Department of Electrical Engineering, University of Roorkee, as a Lecturer. In 1988, he became a Reader. In December 1990, he joined the Department of Electrical Engineering, IIT, New Delhi, India as an Assistant Professor. He became an Associate Professor in 1994 and a Professor in 1997. His fields of interest include power electronics, electrical machines and drives, active filters, static compensators, and analysis and digital control of electrical machines. Prof. Singh is a Fellow of the Indian National Academy of Engineering, Institution of Engineers (India), and Institution of Electronics and Telecommunication Engineers. He is also a Life Member of the Indian Society for Technical Education, System Society of India, and National Institution of Quality and Reliability.

Mahima Agrawal

She was born in Jabalpur (MP), India on August 21, 1980. She received her B.E. degree in Electrical Engineering from Government Engineering College, Jabalpur, India in 2002 and her M.Tech Degree in Power Electronics, Electrical Machines, and Drives from the IIT, Delhi in 2004. She is currently working as an Embedded System Engineer at APC India Private Limited, Bangalore, India. While studying for her M.Tech, she received the IEEE PEDES'96 award. Her areas of interest include UPS and inverters, DSP based systems, power factor correction, high-frequency isolation, and electrical machines and drives.

Sanjeet Dwivedi

He was born in Chhatarpur (M.P.) India in 1968. He received his B.E. (Electrical) degree from Government Engineering College Jabalpur, India, in 1991, his M.Tech. degree with Gold Medal recognition from the University of Roorkee, Roorkee, India in 1999, and his Ph.D. degree from the Indian Institute of Technology, Delhi, India in 2006.

In 1991, he joined Larson and Toubro Ltd. as a Graduate Engineer Trainee. In November 1993 he joined the Department of Electrical Engineering, Indira Gandhi Engineering College, Sagar (M.P.) as a Lecturer. He went on to become Senior Lecturer in 1999, Reader in 2004, and Head of the Department in 2007. His research interests are in areas of digital control of Brushless Motors, sensor reduction techniques in ac drives, high frequency isolated converters and their control, and power quality aspects of ac drives.